IEEE Access
Multidisciplinary | Rapid Review | Open Access Journal

Received August 19, 2020, accepted September 16, 2020, date of publication September 24, 2020, date of current version October 8, 2020.

Digital Object Identifier 10.1109/ACCESS.2020.3026623

Underwater Communication Employing High-Sensitive Magnetic Field Detectors

MAURICE HOTT AND PETER ADAM HOEHER, (Fellow, IEEE)
Faculty of Engineering, Kiel University, 24143 Kiel, Germany

Corresponding author: Maurice Hott (maho@tf.uni-kiel.de)

This was supported by the European Union – European Regional Development Fund (ERDF), the Federal Government and Land Schleswig-Holstein, Germany, through EU.SH Project, under Grant LPW-E/1.2.2/1075.

ABSTRACT Magnetic communication is receiving significant interest in RF-challenging environments. Particularly in underwater environments and underground wireless sensor networks, magnetic communication is an emerging research area. In this paper, a new approach for magnetic underwater communication is presented and evaluated. In this approach, the receiver coil of a conventional magnetic induction communication system is replaced by a high-sensitive low-noise wideband magnetic field sensor. This concept enables a good detection sensitivity and, under certain conditions, an extended communication range. Most magnetic field sensors are small compared to equivalent search coils and offer a high bandwidth. Hence, they can be assembled in order to provide multiple-input multiple-output processing. Based on suitable channel modeling, trade-offs between system parameters are analyzed and the channel capacity is derived. Analytical results are supported by a prototype implementation. Potential application scenarios are studied, where emphasis is on mobile applications.

INDEX TERMS Communication channels, communications technology, magnetic field measurement, magnetic sensors, mobile communication, underwater communication, underwater technology.

I. INTRODUCTION

Oceans cover more than 70 percent of the Earth's surface, but only a fraction of the seabed is already explored. At least locally, new insights can be gained through underwater robotics and sensor networks. Digital communication is a key technology for data exchange between mobile nodes and/or fixed installations, both in near/mid-range and far-range applications. A bottleneck is the lack of fast yet robust wireless underwater communication techniques. Most commercial wireless underwater communication systems are either based on acoustic waves or optical links. Acoustic modems offer the largest communication range among these options, but the bandwidth is small and the latency may be problematic. Reliable acoustic communication is difficult particularly in shallow waters. Multipath propagation causes a large delay spread, and mobility a significant Doppler spread. Optical communication is strongly affected by the visibility between transmitter and receiver, as well as by daylight in shallow water depths.

The associate editor coordinating the review of this manuscript and approving it for publication was Qiong Wu.

A promising alternative for near/mid-range communication is to exploit magnetic fields for digital communication [1]–[8]. Unlike radio waves, which are radiative and hence subject to multipath propagation, operation is in the non-radiative near field. Typically, coils are used both at the transmitter side as well as at the receiver side. The transmitter coil is driven by a modulated AC current. By means of magnetic induction (MI), the information-carrying signal is reproducible at the receiver side. Magnetic near-field communication has distinctive features. Compared to acoustical communication, advantages of MI include a scalable bandwidth over a wider spectral range, a negligible propagation delay, and less susceptibility to surroundings. This technique is insensitive to water turbidity (including surf zones, tidal flow, and rivers), water depth, reflections by materials and surfaces, interference by sound and light, as well as Doppler spread and delay spread. In the non-radiative near field, critical issues like multipath propagation and fading are negligible. Due to the scalable bandwidth, multi-user communication and networking are more efficient. In autonomous underwater vehicle (AUV) and remotely operated vehicle (ROV) applications, acoustic communication is affected

by vibrations of the thrusters. Coils can be integrated into non-metal hulls, whereas acoustic transducers protrude into the water. Furthermore, fast-decaying magnetic fields are more environment-friendly for marine mammals than sound waves. In contrast to optical underwater communication, intervisibility and ambient light are no bottleneck. The pointing and acquisition problem of collimated optical beams does not exist in MI communication. Narrowband relaying is simple because it can be achieved with passive resonant circuits [1]. In summary, communication in harsh environments like shallow water, turbulent water, and harbors is feasible. Magnetic communication is one of the few techniques that work below and simultaneously above the sea surface (or above and simultaneously below the sea bottom). Magnetic fields can be used jointly for communication, localization, energy harvesting, and for tracing metal objects. These synergetic effects are beyond the scope of this contribution.

However, a fundamental physical drawback of MI is the distance law. In the non-radiative near-field regime, the ratio between the received power and the transmitted power is proportional to d^{-6}, whereas in the radiative far-field regime it is d^{-2}. Both figures hold for line-of-sight propagation in air or purified water. In salty waters with conductivity $\sigma_m > 0$, attenuation is even worse for MI. This problem can be relaxed to some extend by using large-size coils (or low frequencies), for example. However, these are bulky and hence not suitable for mobile applications.

In [9], we have presented a novel magnetic communication approach: The receiver-side coil of a classical MI system has been replaced by a high-sensitivity low-noise wideband magnetic field sensor. Related work has independently been published in [10], where the emphasis is on diver communication employing a speech codec, and in [11], [12], where magnetic field detectors are used for localization purposes in air and fluids. This cheap and reliable approach offers several benefits and, under certain circumstances, an extended communication range. In our prototype receiver, several high-sensitive wideband low-noise anisotropic magnetoresistance (AMR) magnetic field sensors are implemented. The resistance of AMR sensors, typically operated in a Wheatstone bridge, is a function of an external magnetic field. Among the advantages is that these magnetic field sensors are very small and suitable for multiple-input multiple-output (MIMO) processing. It should be noted that the measurement principle of magnetic field sensors is not based on MI. Hence, the system performance, as well as the trade-offs between relevant system parameters, are different for the magnetic communication approach under investigation. In this work, detailed underwater channel modeling for magnetic communication employing magnetic field detectors is provided. The terms magnetic field sensor and magnetic field detector are used alternately. Novel contributions include the following aspects:

- The magnetic underwater channel is examined both for a homogeneous water column as well as for shallow water depths and surfaces.
- The trade-offs between relevant system parameters are studied analytically.
- The SNR enhancement by using several sensors is studied.
- Our analysis is supported by an experimental prototype.

The remainder is organized as follows. In Section II, the channel model and the trade-offs between relevant system parameters are studied analytically. A prototype implementation demonstrating the feasibility of the system concept is presented in Section III. Potential applications are suggested in Section IV. Finally, conclusions are drawn in Section V.

II. THEORETICAL ANALYSIS

A. NEAR-FIELD COMMUNICATION

A fundamental advantage of magnetic near-field communication is the insensitivity to reflection/scattering/diffraction caused by the seafloor and other obstacles. However, it is important to note that this characteristic is only valid in the non-radiative near field [13]. The terms ''near field'' and ''far field'' mentioned before describe different spatial areas in antenna technology that surround the radiator. The spatial areas are usually divided into three areas:

- The *reactive near field* is the area in the immediate vicinity of the radiator. In this region, transmission is non-radiative. In the case of a coil, a magnetic field is obtained. Magnetic field lines are closed.
- The *radiating near field* is the transition field, also referred to as the Fresnel region.
- The *far field*, also called the Fraunhofer region, is the area in which an electromagnetic wave propagates in space as a wave. In the far field, magnetic communication suffers from multipath propagation and the associated fading at the receiver side.

The boundaries between the individual regions depend on the wavelength λ and are radiator-dependent. Frequently, the reactive near field is defined for distances up to $\lambda/(2\pi)$ around the radiator and the far field is said to start at about 4λ. The distance

$$d_{\mathrm{nf}} = \frac{\lambda}{2\pi} = \frac{c_{\mathrm{m}}}{2\pi f} \tag{1}$$

at which the non-radiative near field passes to the radiating near field is an essential parameter with respect to system design. This boundary depends on the frequency f of the transmitted signal and the speed of light c_{m} in the transmission medium.

The speed of light is a material-dependent parameter and can be calculated as follows:

$$c_{\mathrm{m}} = \frac{1}{\sqrt{\mu\epsilon}} = \frac{1}{\sqrt{\mu_0\mu_{\mathrm{r}}\epsilon_0\epsilon_{\mathrm{r}}}} = \frac{c_0}{\sqrt{\mu_{\mathrm{r}}\epsilon_{\mathrm{r}}}}, \tag{2}$$

where c_0 describes the speed of light in vacuum, μ the absolute permeability, μ_{r} the relative permeability, $\mu_0 = 4\pi \cdot 10^{-7}$ H/m the vacuum's absolute permeability, ϵ the absolute permittivity, ϵ_{r} the relative permittivity and $\epsilon_0 = 8.85 \cdot 10^{-12}$ F/m the vacuum's absolute permittivity.

The relative permeability of water is similar to the one of air and is defined as $\mu_\mathrm{r} = 1$. The relative permittivity in water is different from the one of air and is a frequency-, temperature-, and salinity-dependent parameter. For pure water with a temperature of 10 °C and a signal frequency between 0 Hz and 1 GHz, the permittivity is about $\epsilon_{\mathrm{r,\,water}} \approx 84$ [14]. The relative permittivity for water drops down slightly for increasing temperature and/or salinity (shielding effect) [15]. However, this effect is very small for variations in temperature and salinity of common water types, so that it can be neglected here. For example, given a signal frequency of $f = 100$ kHz and a speed of light of $c_\mathrm{water} = 3.27 \cdot 10^7$ m/s in pure water with $\epsilon_r = 84$ yields $d_\mathrm{nf} = 52$ m. This value represents the maximum non-radiative near-field communication distance for the considered underwater channel and transmission frequency, independent of transmitter power and receiver sensitivity.

B. CHANNEL MODELING FOR A HOMOGENEOUS WATER COLUMN

According to Biot-Savart's law, for a planar coil with N_w windings, excitation current I, and azimuth angle α with respect to the main coil axis, at a distance d the magnetic flux density can be expressed in non-conductive environments (like air) as

$$B = \frac{\mu_0 N_\mathrm{w} I r^2 \cos(\alpha)}{2(r^2 + d^2)^{3/2}}, \tag{3}$$

where $r = (r_\mathrm{o} + r_\mathrm{i})/2$ with r_o being the outer and r_i the inner radius of the coil. Note that for $d \gg r$ the magnetic flux density is proportional to $1/d^3$.

All known wireless communication principles are subject to high signal attenuation under water, which makes communication at reasonable data rates very difficult. In the case of magnetic communication in conductive media such as seawater, an additional signal attenuation is caused by eddy currents. Eddy currents produce a negative moment that changes the transmitted moment and the field distribution. The signal attenuation is a function of the skin depth δ. For good conductors, the well-known approximation for the skin depth applies:

$$\delta = \frac{1}{\sqrt{\pi f \mu \sigma}}. \tag{4}$$

For bad conductors, e.g. seawater, a more general expression must be used [16]:

$$\delta = \frac{1}{2\pi f \sqrt{\frac{\mu_\mathrm{m}\epsilon_\mathrm{m}}{2}\left(\sqrt{1 + \frac{\sigma_\mathrm{m}^2}{(2\pi f)^2 \epsilon_\mathrm{m}^2}} - 1\right)}}. \tag{5}$$

The equation shows that the signal frequency f, the magnetic permeability μ_m, the permittivity ϵ_m, and the conductivity of the transmission medium σ_m contribute to the skin depth. For a homogeneous conductive transmission medium, the eddy-current-related signal attenuation can be expressed by the term

$$e^{-\frac{\sqrt{d^2+r^2}}{\delta}}. \tag{6}$$

Altogether, (3) can be extended as

$$B = \frac{\mu_0 N_\mathrm{w} I r^2 \cos(\alpha)}{2(r^2 + d^2)^{3/2}} e^{-\frac{\sqrt{d^2+r^2}}{\delta}}. \tag{7}$$

This manifests that the magnetic flux density decreases with increasing signal transmission frequency and/or conductivity. The conductivity of water is mainly given by the number of ions and increases with salt concentration. The main types of ions in seawater are chlorine and sodium. The salinity for different water types like tap water, lake water, or seawater varies widely. In general, a distinction is made between freshwater (≤ 0.1 %), brackish water (between 0.1 % and 1 %), and saline water (≥ 1 %). The Baltic Sea has an average salt content of ≈ 0.8 %, which is far below the average salt content of the oceans with ≈ 3.5 %. The relationship between the salinity and the electrical conductivity has been studied in [17].

To specify the decay of the magnetic field between transmitter and receiver in the presence of a certain homogeneous medium, the magnetic loss is derived from (7) as

$$\begin{aligned} \mathrm{ML}_\mathrm{hom} &= 20\log_{10}\left(\frac{2(r^2 + d^2)^{3/2}}{e^{-\frac{\sqrt{d^2+r^2}}{\delta}}}\right) - 20\log_{10}\left(\frac{2r^3}{e^{-\frac{r}{\delta}}}\right) \\ &= 20\log_{10}\left(\frac{2(r^2 + d^2)^{3/2} e^{-\frac{r}{\delta}}}{2r^3 e^{-\frac{\sqrt{d^2+r^2}}{\delta}}}\right). \end{aligned} \tag{8}$$

It represents the loss of the magnetic field amplitude in dB for an optimal alignment ($\alpha = 0$) depending on the transmitter coil radius and the skin depth of the medium and is independent of the number of windings and the coil current. The ML is normalized to the magnetic field strength in the physical center of the coil, constituting $d = 0$.

Fig. 1 depicts the magnetic loss for magnetic communication as a function of distance for the conductivity of air, tap

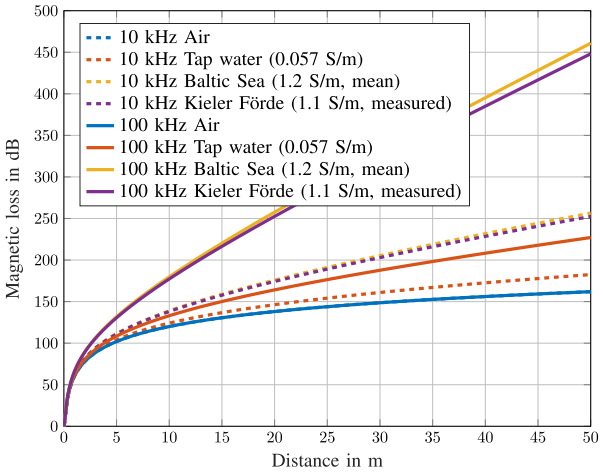

FIGURE 1. Magnetic loss as a function of distance for different homogeneous media.

water, Kiel Fjord water, and Baltic Sea water. The magnetic loss is plotted for the signal frequencies 10 kHz and 100 kHz.

For $d \gg r$, in non-conductive environments like air the magnetic loss is proportional to d^3 and is independent of the signal frequency. For conductive media, i.e. $\sigma > 0$, the magnetic loss further increases with higher conductivity and signal frequency. The plot also shows that the influence of increasing conductivity can be compensated by reducing the signal frequency.

C. MAGNETIC LOSS FOR NEAR-SURFACE COMMUNICATION

Conventional models for calculating the performance of magnetic communication systems are based on the assumption of a homogeneous, infinitely extended transmission medium. This assumption neither holds near the surface nor near the bottom. There are approaches in the area of magneto-inductive underground communication, which model the signal propagation in heterogeneous media, see for example [18]. Frequently, however, only the distance-dependent variations of the medium between the sender and receiver are considered. For the case of underwater communication, the vertical variation of the medium is important, whereby the interface between water and air represents the greatest change in the medium properties. If the transmitter or receiver is located at a relatively shallow depth below the water surface and the communication distance is sufficiently large, the magnetic field lines partly pass through the air. Consequently, these are less attenuated, which leads to an underestimation of the communication range by most existing models.

In [19], a scenario is examined where a coil is placed exactly on the boundary between two media. The coil is simplified as a magnetic dipole in the referenced publication. Consequently, this approximation is valid for distances much larger than the coil radius ($d \gg r$). Moreover, this equation supports only a 2-layer model and is not able to take into account a coil placed at different depths below the sea surface. For this reason, we applied a finite element method (FEM) analysis using COMSOL Multiphysics. In this context, a deep water scenario and a shallow water scenario are investigated.

1) DEEP WATER MODEL

In deep water, where the water depth is much larger than the communication distance, the properties of the seabed are negligible. This makes the examination of a 2-layer model sufficient. We assume that the main coil axis is aligned in parallel to the sea surface. Different coil depths are emulated. The scenario is illustrated in Fig. 2.

Fig. 3 shows the corresponding results of the FEM calculation for selected communication depths. For seawater, a conductivity of $\sigma = 1.2$ S/m is assumed. The signal frequency is selected as $f = 100$ kHz. As a reference, the magnetic loss for homogeneous air and seawater with an infinite expansion is shown. The results support the assumption that the magnetic loss gradually increases with depth under the sea surface. It can be seen that all curves for the different water depths initially follow the same function. When the distance is about twice as large as the depth below the sea surface, the magnetic loss curve converges to the d^3 distance law. These findings confirm that known homogeneous channel models underestimate the channel when the depth is less than the transmission distance.

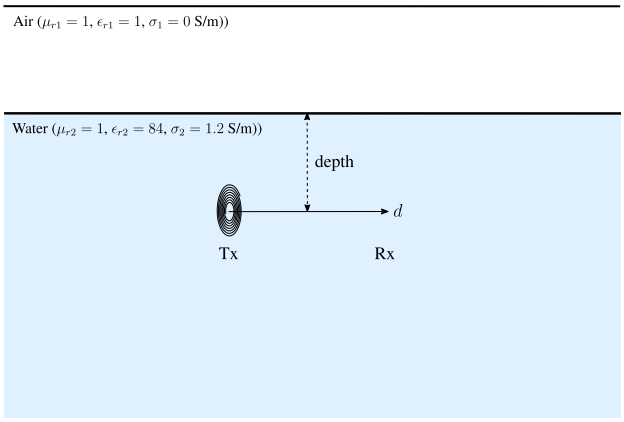

FIGURE 2. Deep water 2-layer model for communication near the water surface.

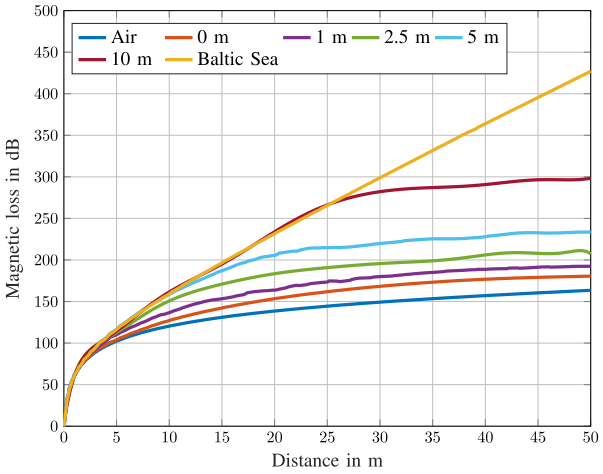

FIGURE 3. Magnetic loss as a function of distance d in deep water for different depths given the scenario in Fig. 2. The signal frequency is specified as $f = 100$ kHz and the conductivity is $\sigma = 1.2$ S/m.

2) SHALLOW WATER MODEL

In shallow waters, the communication distance can be smaller than the water depth. In this case the properties of the seabed should be considered in the model for an accurate calculation of the magnetic loss. Hence, a 3-layer FEM model is developed, which represents the media air, water and the seabed. Fig. 4 illustrates the scenario and shows the chosen magnetic and electrical parameters of air, water and the seabed. The main coil axis is aligned in parallel to the water surface and is located at half the water depth. The signal frequency is $f = 100$ kHz.

Fig. 5 shows calculated magnetic loss based on the FEM analysis as a function of distance for different water depths.

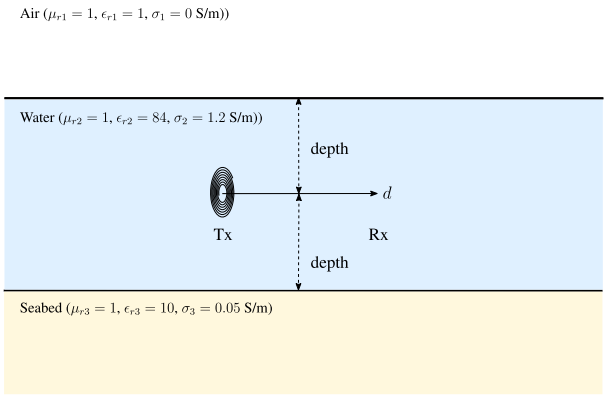

FIGURE 4. Shallow water 3-layer communication model.

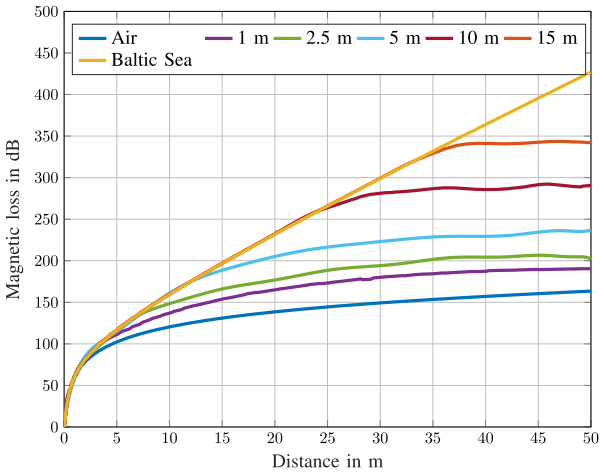

FIGURE 5. Magnetic loss as a function of distance d in shallow water for different depths given the scenario in Fig. 4. The signal frequency is specified as $f = 100$ kHz and the conductivity is $\sigma = 1.2$ S/m.

As expected, the magnetic loss in deeper waters increases faster with distance. In direct comparison to the results of the deep water 2-layer model in Fig. 3, it can be seen that the seabed slightly reduces the magnetic loss compared to seawater due to its greater skin depth. Overall, the use of a multi-layer model can improve the accuracy of the results in both scenarios. It should be noted that the assumption of a homogeneous infinitely extended medium in low communication depths and shallow water scenarios leads to an underestimation of the channel.

D. TRADE-OFFS BETWEEN SYSTEM PARAMETERS

In this section, the influence of adjustable system parameters on the proposed magnetic communication system is investigated. The adjustable parameters are separately investigated for the transmitter and receiver side. The analysis serves as a design guide for magnetic communication systems. The maximum communication distance under consideration is set to 50 m. This corresponds approximately to the non-radiative near-field boundary in water for a signal frequency of 100 kHz.

1) SNR

The signal-to-noise ratio (SNR) is a fundamental parameter in communications, besides the bandwidth. The SNR is determined by the ratio between the received signal power and the noise power, or the corresponding root mean square (RMS) voltages at the detector output:

$$\mathrm{SNR} = \frac{P_\mathrm{S}}{P_\mathrm{N}} = \frac{U^2_{\mathrm{RMS,\,S}}}{U^2_{\mathrm{RMS,\,N}}}. \tag{9}$$

To calculate the RMS voltage of the wanted signal $U_{\mathrm{RMS,\,S}}$, Eqn. (3) can be used, which gives the magnetic flux density as a function of the link distance for a homogeneous media. By additionally considering the sensitivity S of the magnetic field sensor and the amplifier gain g, the RMS voltage at the detector output can be determined:

$$U_{\mathrm{RMS,\,S}} = gSB_{\mathrm{RMS}}. \tag{10}$$

Since $U_{\mathrm{RMS,\,S}} \sim B$ applies, $P_\mathrm{S} \sim B^2$ holds. This clearly demonstrates that the power decreases by d^{-6}.

The RMS noise voltage $U_{\mathrm{RMS,\,N}}$ can be calculated by summing of all noise sources. For this purpose, all contributing circuit components must be taken into account. For the proposed communication system, the AMR sensor and the instrumentation amplifier are the main noise sources on the receiver side:

$$U_{\mathrm{RMS,\,N}} = gE_{\mathrm{RMS,\,AMR}} + E_{\mathrm{RMS,\,AMP}}. \tag{11}$$

Note that the noise of the AMR sensor is amplified by the instrumentation amplifier.

2) TRANSMITTER DESIGN

In Fig. 1 the magnetic loss is shown for different frequencies and conductivities as a function of the distance. The magnetic loss describes the attenuation of the signal which occurs in the link between transmitter and receiver. To ensure that the SNR at the receiver side is still sufficient, the amplitude of the generated signal must be sufficiently large. In the case of magnetic communication, this signal is generated by a coil. The properties of the coil and the current flowing through the coil indicate the strength of the magnetic field generated, as shown in (3). For a better understanding the number of windings, the current through the coil and the coil radius can be substituted in the magnetic moment

$$m = N_\mathrm{w} I \pi r^2. \tag{12}$$

To maximize the magnetic moment generated by the coil, the number of turns, the current, and/or the area enclosed by the coil can be increased. The magnetic moment is proportional to the square of the coil radius. However, it should be noted that additional power is required to keep the current through the coil constant, as the length of the conductor, and thus the electrical resistance increases. The same applies when the number of windings is increased. The coil current does not affect the other parameters of the magnetic moment.

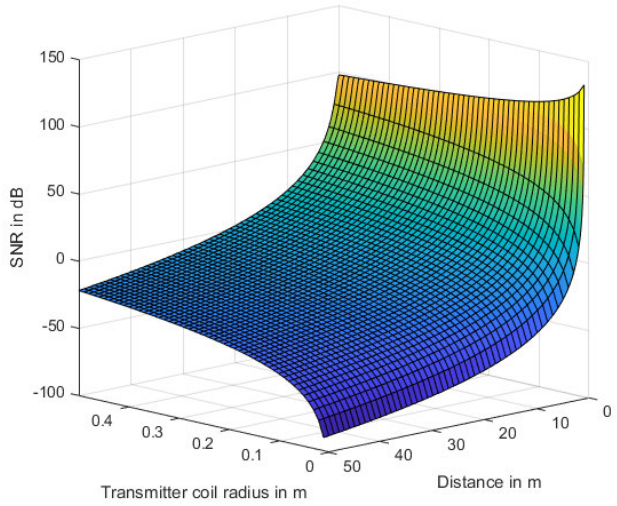

FIGURE 6. SNR at the sensor output as a function of the radius of the transmitter coil and the distance between transmitter and receiver.

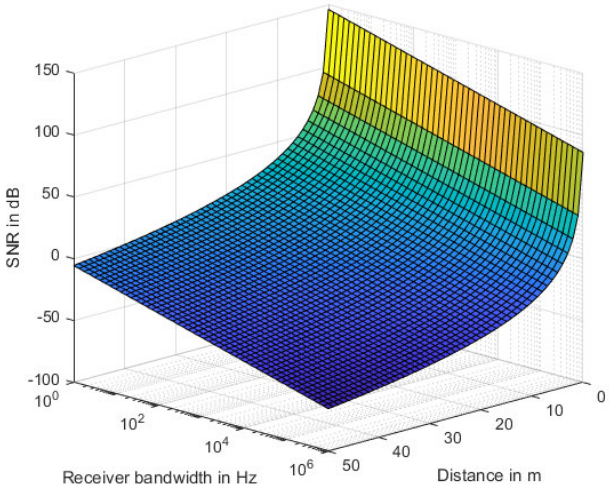

FIGURE 7. SNR at the sensor output as a function of the receiver bandwidth and the distance between transmitter and receiver.

To enable high coil currents, the transmitter coil can be operated in a resonant circuit. For this purpose, a component with capacitive characteristics, such as a capacitor, is connected in parallel (parallel resonant circuit) or in series (series resonant circuit) with the coil. This provides a frequency where the reactances of coil and capacitor cancel each other out $X_C = X_L$, which is called electrical resonance. As a result, the maximum coil current I in a series resonant circuit at the resonant frequency f_r is limited only by the Ohmic resistance of the coil and the internal resistance of the source:

$$I = \frac{V}{\sqrt{R^2 + (X_L - X_C)^2}}. \tag{13}$$

In this way, strong alternating magnetic fields can be generated efficiently. The so-called quality factor is an expression of the ratio between the reactance of the coil or capacitor and the Ohmic resistance at the resonant frequency: $Q = X_L/R$. However, a low resistance is at the expense of bandwidth which is defined as $\Delta f = f_r/Q$. The upper and lower cut-off frequency is determined by the 3 dB limits of the quality curve of the resonant circuit. This results in a trade-off between coil current and bandwidth.

Fig. 6 shows the SNR at the receiver side as a function of the radius of the transmitter coil and a given distance between transmitter and receiver. The amplitude of the coil current is set to $I = 7$ A and the number of windings to $N_\mathrm{w} = 100$. The analysis is performed for air respectively pure water with a perfect alignment ($\alpha = 0$) and a bandwidth of $\Delta f = 5.4$ kHz. It is noticeable that the SNR decreases with an increasing radius for small transmission distances. This can be explained by the fact that the distance from the coil axis to the current-carrying conductor increases. For larger distances ($d \gg r$), the enlargement of the radius has the effect of an increasing SNR. It should be considered that the frequency of the alternating field in conductive materials also contributes to attenuation, this must also be taken into account in the system design.

3) RECEIVER DESIGN

The receiver performance is limited by the magnetic field sensor sensitivity and the total noise of the detector circuit. The total noise results from the noise contributions of all circuit components and is a bandwidth-dependent value. The noise characteristic of a component is defined by the noise voltage density E_N in the data sheet, which has the unit $\frac{\mathrm{V}}{\sqrt{\mathrm{Hz}}}$. The RMS noise voltage $E_{\mathrm{RMS,\,N}}$ can be calculated by using the equivalent noise bandwidth (ENBW) Δf of the receiver:

$$E_{\mathrm{RMS,\,N}} = E_\mathrm{N}\sqrt{\Delta f}. \tag{14}$$

ENBW can be obtained by the filter 3 dB frequency $f_{3\,\mathrm{dB}}$ and the steepness s of the used filter type, which compensates the filter characteristic: $\Delta f = s \cdot f_{3\,\mathrm{dB}}$. For a brick wall filter, $\Delta f = f_{3\,\mathrm{dB}}$ applies. For example, if a pole filter with one pole is used, the value is defined as $s = 1.57$.

Fig. 7 shows the expected SNR on the receiver output as a function of distance and the communication bandwidth. As expected, the SNR decreases with increasing bandwidth and distance. Therefore, the bandwidth efficiency should be taken into account in the system design, which describes the information rate that can be transmitted over a given bandwidth for the communication system.

To describe the performance of a magnetic field sensor, the so-called sensibility B_min is taken as a measure. The sensibility describes the sensitivity of the sensor in relation to its inherent noise. In this paper, the sensibility is defined by the magnetic flux density at which the RMS signal level is equal to the RMS noise level (SNR = 0 dB). Fig. 8 shows the relationship between communication range and sensibility for different water types. It is important to note that the maximum range refers to an SNR of 0 dB and is not a general upper limit for the sensitivity of the sensor. If the overall

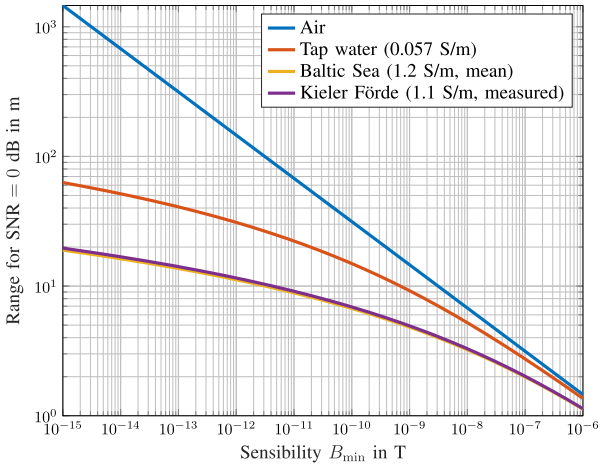

FIGURE 8. Communication range for an SNR of 0 dB as a function of the sensibility $B_{\min}$ of the magnetic field detector for selected water types.

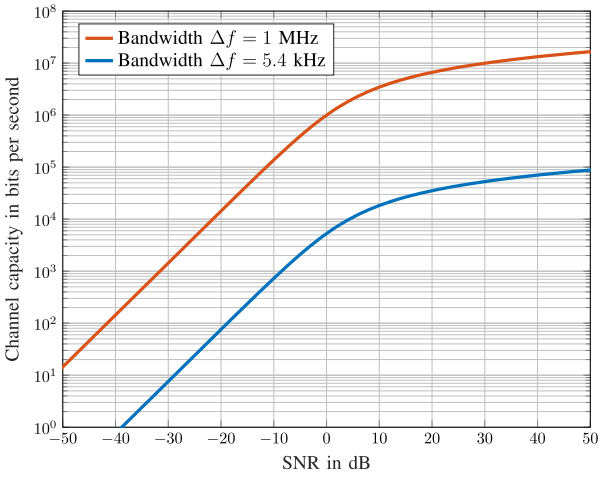

FIGURE 9. Channel capacity as a function of SNR for a bandwidth of 5.4 kHz and 1 MHz.

detector would be able to operate at an SNR of less than 0 dB, for example by means of low-rate channel coding, the curves in Fig. 8 would move towards larger ranges.

4) CHANNEL CAPACITY

The channel capacity represents the maximum information rate (in b/s) at which information can be transmitted quasi error-free over a channel. The calculation of the channel capacity varies depending on the type of transmission channel. For the magnetic communication between a coil and an AMR based receiver, the channel distortions can be modeled by additive white Gaussian noise (AWGN) in good approximation. Thus, the single-input single-output channel capacity can be calculated by using the Shannon–Hartley theorem:

$$C = \Delta f \cdot \log_2\left(1 + \frac{P_S}{P_N}\right) = \Delta f \cdot \log_2\left(\frac{P_S + P_N}{P_N}\right), \quad (15)$$

where Δf is the channel bandwidth, P_S the received signal power and P_N the noise power. This equation holds for Gaussian-distributed channel input symbols. The channel capacity for a given distance can be determined by measuring the total signal, which is a superposition of the wanted signal plus noise (numerator) and by measuring the noise only (denominator). Fig. 9 shows the channel capacity as a function of SNR for different bandwidths. The blue curve depicts the channel capacity for a bandwidth of 5.4 kHz. The red curve represents the channel capacity for a bandwidth of 1 MHz, which corresponds to the maximum bandwidth of the AMR sensor used in the prototype. It can be seen that the channel capacity for an SNR of 0 dB corresponds to the bandwidth and grows for an increasing SNR. Thus, the red curve is shifted by the factor 185 with regard to the blue curve. It should be remembered that the receiver noise also increases with the bandwidth (see Fig. 7) and the SNR decreases for that reason. With MIMO signaling the channel capacity can be boosted.

5) SNR ENHANCEMENT

An improved SNR at the receiver side leads to fewer transmission errors and thus increases the channel capacity of the transmission channel. In addition to boosting the transmission power, the noise can also be reduced by using a smaller bandwidth for a better SNR. Another approach to minimize the receiver noise exploits the statistical independence of the noise. While the signal power increases linearly by averaging over n sequences, the noise power increases only with the square root of the number of averaged sequences. This improves the SNR according to the central limit theorem by the factor

$$\frac{n}{\sqrt{n}} = \sqrt{n}. \quad (16)$$

If the channel noise is very small, approximately all noise contributions at the receiver are produced in the detector circuit. In this case, spatial averaging of the measured signal is a preferable alternative to time averaging. This can be achieved by using $n > 1$ magnetic field sensors for signal detection. The symbol rate remains the same for physical averaging, whereas the symbol rate decreases for time-based averaging. Due to the small footprint of the AMR, a large number of sensors can be mounted on a mobile-friendly receiver circuit for realizing an SNR enhancement. This aspect is investigated by using the developed prototype system introduced in Section III.

III. PROTOTYPE IMPLEMENTATION

In this section, the suitability of the communication concept for underwater environments is verified. For this purpose, a small-scale underwater communication system is developed (Fig. 10), and measurements are taken in the Kiel Fjord, an area in the southwestern region of the Baltic Sea, and analyzed.

The magnetic communication approach under investigation is based on a direct measurement of the magnetic field,

FIGURE 10. Small-scale magnetic communication experiment setup. The transmitter circuit including the coil is shown on the left, the magnetic field detector circuit on the right. Transmitter and receiver are pressure-neutral encapsulated.

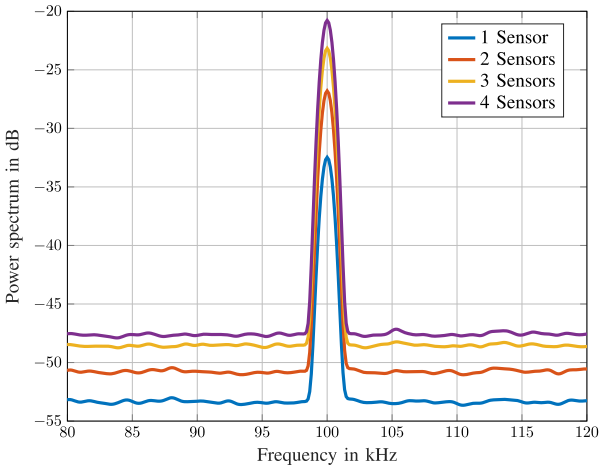

FIGURE 11. Power spectrum measured for sensor array with a maximum number of four sensors working jointly.

which is produced by a transmitter coil. The setup includes a planar transmitter coil with a radius of $r = 1.6$ cm and $N_w = 10$ windings, that operates in resonant mode and is driven by a half-bridge inverter. The resonant frequency is tuned to 100 kHz. The coil current amplitude is chosen as $I = 3$ A. The receiver coil of a conventional MI communication system is replaced by a custom-made detector circuit, which is based on a Sensitec AFF755 high-sensitive wideband low-noise AMR magnetic field sensor with a size of about 25 mm^2 including packing. The typical sensitivity of this sensor is specified as 15 $\frac{\text{mV/V}}{\text{kA/m}}$, which allows measurements of weak magnetic flux densities in the frequency range from 0 Hz up to 1 MHz. The sensor signal is amplified by a wideband low-noise instrumentation amplifier with a fixed gain-factor of 2000. The developed small-scale prototype achieves for the resonant frequency an SNR of 12 dB at a distance of 80 cm between transmitter and receiver. For an AWGN channel this corresponds to a channel capacity of 21.64 kb/s.

As theoretically shown in Section II-D5, an SNR enhancement can be achieved by using multiple sensors for spatial averaging according to the central limit theorem. Here, the influence of the physical number of magnetic field sensors working jointly on the SNR is investigated practically. For this purpose a detector circuit with four independently operating AMR sensors was developed. The circuit includes four AMR sensors and four instrumentation amplifiers. The signal of the AMR sensors is amplified by one instrumentation amplifier each. This allows separate measurement data acquisition for each sensor. The measuring signal can be digitally summed and evaluated for a varying number of sensors. In the measurement setup, a signal of 100 kHz was generated with a transmitting coil. This signal was measured with the detector array and digitally evaluated.

Fig. 11 presents the power spectrum as a result of the combination of the signals from a different number of sensors. The spectrum depicts that the signal power increases by 6 dB when doubling the number of sensors. The noise level on the other hand only increases by 3 dB when doubling the number of sensors. This gives a total SNR gain of 3 dB when doubling the number of sensors which are working jointly. Since the measurement results are in accordance with the central limit theorem, the magnetic channel noise can be neglected in the considered frequency range. Thus, spatial averaging with a large number of sensors is as a useful way to enhance the SNR significantly.

IV. POTENTIAL APPLICATIONS

In conventional MI communication, the same coil can be used as both transmitter and receiver (transceiver). Thus, by its basic concept, an MI system offers bidirectional data transmission. If one coil is replaced by a magnetic field sensor, the bidirectionality is lost at the cost of newly obtained advantages. However, there are many scenarios in which only unidirectional communication is needed and other interests, such as receiver size or weight, have priority. The benefits of a small, lightweight receiver introduce new possibilities in the field of underwater communication. But even in scenarios where bidirectional communication is required, an additional integration of a magnetic field sensor in the transmitter and receiver circuit can provide further advantages, like an SNR improvement. Furthermore, a broadband signal detection is enabled. Hence, the received signals are not limited by the tuned resonant frequency of the transmitter coil. In the following, two scenarios are presented, which are enabled by the use of one or several high-sensitive low-noise wideband magnetic field sensors applied for data reception.

A. DEPLOYMENT BETWEEN STATIONARY AND MOBILE NODE(S)

Fig. 12 illustrates a communication scenario for coastal and harbor areas, where common techniques have severe problems to establish a reliable data transmission. Here, acoustic communication struggles with reflections from quay

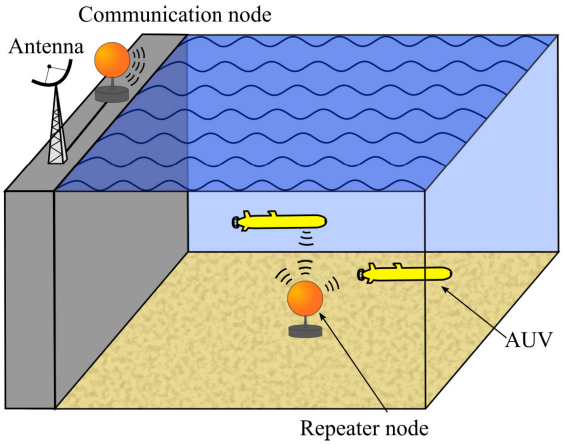

FIGURE 12. Scenario 1: Inshore communication using a powerful land transmitter and repeater node anchored on the seabed. 3D magnetic field sensors in the AUVs ensure a permanent downlink. Optionally, a small 3D transmitter coil integrated into the AUVs serves as a transmitter for a temporary uplink with short communication range.

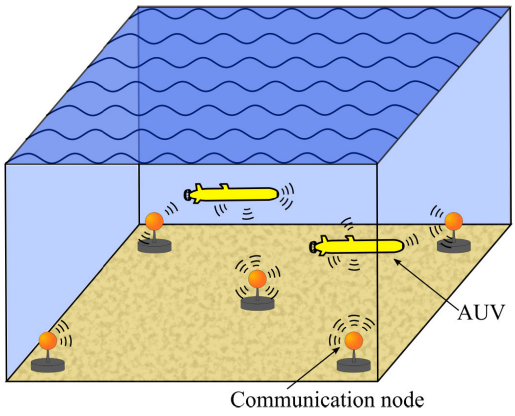

FIGURE 13. Scenario 2: Offshore communication using several low power communication nodes anchored on the seabed. The communication nodes and AUVs provide a 3D coil as transmitter and a 3D magnetic field detector as receiver.

walls and optical communication with poor visibility conditions in the port basin. A promising solution could be magnetic communication, especially by employing magnetic field detectors. In this case, a large onshore 3D coil with a permanent power supply can generate a strong magnetic signal. Thereby, magnetic near-field propagation is not affected by the air-water boundary. In addition, a communication node equipped with a large 3D coil and a magnetic detector is placed inshore, which acts as a repeater. Ideally, this transceiver is supplied with permanent power. The AUVs are equipped with a 3D magnetic field detector, which enables a continuous downlink. A small 3D transmitter coil with a short communication range can additionally be used. This ensures a temporary uplink, for example when an AUV is located close to a communication node. Furthermore, this allows an AUV to continuously receive data and transmit the collected data during the periods when the node is within range of the transmitting coil. A further advantage by using magnetic field detectors as a receiver is that the transmitter coils can be tuned on different resonant frequencies. This enables the full bandwidth for all transmitters. In addition, this allows the associated transmitter to be distinguished by knowing the corresponding frequency without the use of identification codes. Besides, this simplifies the realization of localization algorithms. The wideband receiver allows all participants to observe multiple signals simultaneously.

B. DEPLOYMENT BETWEEN MOBILE NODES

Fig. 13 presents an offshore communication scenario for data transmission and localization purposes. Here, spatially distributed battery-operated low-power communication nodes are placed on the seafloor. Each communication node provides a magnetic field detector as a receiver and a transmitter unit based on a small 3D coil. The transmitter resonant circuits are tuned to different frequencies so that the transmission frequency is unique for each communication node. Due to the large bandwidth of the magnetic field detector, each network participant can observe all transmitted signals simultaneously and discriminate the signal sources. This is a great advantage compared to MI communication where a small bandwidth has to be shared when several participants are active. As in the first scenario, the AUVs are equipped with a 3D magnetic field detector, which enables a continuous downlink. A small 3D transmitter coil with a short communication range is used to ensure a range-limited temporarily uplink connection.

In summary, the advantages of using a wideband magnetic field sensor are:

- Each node can use the full transmitter bandwidth since the transmission frequencies are divided into the bandwidth from 100 Hz to 1 MHz, for example.
- Each node can operate as a repeater.
- No identification code is needed and localization is simplified, due to unique transmit frequencies.
- Only small coils have to be integrated into mobile nodes (AUVs or ROVs) if an uplink is needed.

V. CONCLUSION

In this work, we introduce a new approach for underwater communication, where the receiver coil of a conventional MI communication system is replaced by a high-sensitive low-noise wideband magnetic field sensor. A detailed theoretical analysis of the magnetic underwater communication channel is made for homogeneous water columns, extended by an FEM analysis for communication near water surfaces. In this context, the influence of the water depth on the magnetic loss for magnetic communication is examined. Besides, the adjustable parameters of both the transmitting and the receiving side is elaborated and the influence of these parameters are graphically presented. The results provide a guide for the design of a magnetic communication system. A small-scale prototype system for magnetic communication is presented, which justifies the theoretical analysis.

The results are supported by first measurements that are taken in the Kiel Fjord. It is shown that a further increase of the SNR is possible by combining the signal of multiple sensors, which operate simultaneously. In addition, two underwater scenarios suitable for magnetic communication are pointed out. In these scenarios, the use of magnetic field detectors offers some advantages with respect to communication. Thereby, the large bandwidth of the detector enables simultaneous detection of signals from multiple transmitters without interference. Furthermore, the same sensor can be utilized for positioning and localization purposes. In summary, the findings show that magnetic field communication from a transmitter coil to a magnetic field sensor like an AMR is a promising candidate for low- to mid-range communication purposes in mobile underwater applications, where a small receiver size is required.

REFERENCES

[1] Z. Sun and I. F. Akyildiz, "Magnetic induction communications for wireless underground sensor networks," *IEEE Trans. Antennas Propag.*, vol. 58, no. 7, pp. 2426–2435, Jul. 2010.
[2] J. I. Agbinya, *Principles of Inductive Near Field Communications for Internet of Things*. Denmark, U.K.: River, 2011.
[3] M. Masihpour, "Cooperative communication in near field magnetic induction communication systems," Ph.D. dissertation, Univ. Technol. Sydney, Sydney, NSW, Australia, 2012.
[4] M. C. Domingo, "Magnetic induction for underwater wireless communication networks," *IEEE Trans. Antennas Propag.*, vol. 60, no. 6, pp. 2929–2939, Jun. 2012.
[5] I. F. Akyildiz, P. Wang, and Z. Sun, "Realizing underwater communication through magnetic induction," *IEEE Commun. Mag.*, vol. 53, no. 11, pp. 42–48, Nov. 2015.
[6] S. Kisseleff, "Advances in magnetic induction based underground communication systems," Ph.D. dissertation, Friedrich-Alexander-Univ., Nuremberg, Germany, 2017.
[7] S. Kisseleff, I. F. Akyildiz, and W. H. Gerstacker, "Survey on advances in magnetic induction-based wireless underground sensor networks," *IEEE Internet Things J.*, vol. 5, no. 6, pp. 4843–4856, Dec. 2018.
[8] Y. Li, S. Wang, C. Jin, Y. Zhang, and T. Jiang, "A survey of underwater magnetic induction communications: Fundamental issues, recent advances, and challenges," *IEEE Commun. Surveys Tuts.*, vol. 21, no. 3, pp. 2466–2487, 3rd Quart., 2019.
[9] M. Hott, P. A. Hoeher, and S. F. Reinecke, "Magnetic communication using high-sensitivity magnetic field detectors," *Sensors*, vol. 19, no. 15, p. 3415, Aug. 2019.
[10] B. A. Belyaev, A. N. Babitskii, N. M. Boev, A. V. Izotov, A. A. Sushkov, E. V. Korolev, and A. V. Burmitskikh, "Compact non-linear power amplifier for wideband underwater and underground near-field magnetic communication systems," in *Proc. Int. Siberian Conf. Control Commun. (SIBCON)*, Apr. 2019, pp. 1–5.
[11] C. Hu, M. Li, S. Song, W. Yang, R. Zhang, and M. Q.-H. Meng, "A cubic 3-Axis magnetic sensor array for wirelessly tracking magnet position and orientation," *IEEE Sensors J.*, vol. 10, no. 5, pp. 903–913, May 2010.
[12] S. Carrella, I. Kuncup, K. Lutz, and A. König, "3d-localization of low-power wireless sensor nodes based on amr-sensors in industrial and ami applications," *Proc. Sensoren und Messsysteme*, 2010.
[13] H. Guo, "Performance analysis of near-field magnetic induction communication in extreme environments," *Prog. Electromagn. Res. Lett.*, vol. 90, pp. 77–83, Dec. 2020.
[14] D. G. Archer and P. Wang, "The dielectric constant of water and Debye-Hückel limiting law slopes," *J. Phys. Chem. Reference Data*, vol. 19, no. 2, pp. 371–411, 1990.
[15] N. Gavish and K. Promislow, "Dependence of the dielectric constant of electrolyte solutions on ionic concentration: A microfield approach," *Phys. Rev. E, Stat. Phys. Plasmas Fluids Relat. Interdiscip. Top.*, vol. 94, no. 1, Jul. 2016, Art. no. 012611.
[16] E. C. Jordan and K. G. Balmain, *Electromagnetic Waves Radiating Systerm*. Upper Saddle River, NJ, USA: Prentice-Hall, 1968.
[17] N. P. Fofonoff, "Algorithms for the computation of fundamental properties of seawater," in *Proc. Unesco*, Oct. 1983, pp. 6–14.
[18] S. Kisseleff, I. F. Akyildiz, and W. H. Gerstacker, "Digital signal transmission in magnetic induction based wireless underground sensor networks," *IEEE Trans. Commun.*, vol. 63, no. 6, pp. 2300–2311, Jun. 2015.
[19] J. R. Wait, "Mutual coupling of loops lying on the ground," *Geophysics*, vol. 19, no. 2, pp. 290–296, Apr. 1954.

MAURICE HOTT received the M.Sc. degree in electrical engineering from the Institute of Electrical Engineering and Information Technology, University of Kiel, Kiel, Germany, in 2017. He is currently pursuing the Dr.Ing. (Ph.D.) degree in electrical engineering with the University of Kiel. Since 2017, he has been working as a Research Assistant with the Chair of Information and Coding Theory, University of Kiel. Within the EU.SH project Mobile Autonomous Underwater Vehicles (MAUS) started in 2019, he is working on a novel magnetic communication link between autonomous underwater vehicles. His research interests include digital communication for sensor networks and mobile vehicles exploiting modulated magnetic fields in harsh environments. In his master thesis, he developed innovative signal processing algorithms for sensor arrays in the field of radar technology. He received the ARGUS Science Award 2018.

PETER ADAM HOEHER (Fellow, IEEE) received the Dipl.Ing. (M.Sc.) degree in electrical engineering from RWTH Aachen University, Aachen, Germany, in 1986, and the Dr.Ing. (Ph.D.) degree in electrical engineering from the University of Kaiserslautern, Kaiserslautern, Germany, in 1990. From 1986 to 1998, he was with the German Aerospace Center (DLR), Oberpfaffenhofen, Germany. From 1991 to 1992, he was on leave with AT&T Bell Laboratories, Murray Hill, NJ, USA. He joined the University of Kiel, Germany, in 1998, where he is currently a Full Professor of electrical and information engineering. His research interests include communication theory and applied information theory with applications in wireless radio communications, optical wireless communications, molecular communications, underwater communications, and simultaneous wireless information and power transfer. Since 2014, he has been contributing to decoding and detection that include reliability information. From 1999 to 2006, he served as an Associate Editor for the IEEE TRANSACTIONS ON COMMUNICATIONS.